Microfluidics-Based Single-Cell Functional Proteomics for Fundamental and Applied Biomedical Applications

Jing Yu, Jing Zhou, Alex Sutherland, Wei Wei, Young Shik Shin, Min Xue, and James R. Heath

Division of Chemistry and Chemical Engineering, California Institute of Technology, Pasadena, California 91125; email: heath@caltech.edu

Annu. Rev. Anal. Chem. 2014. 7:275–95

First published online as a Review in Advance on June 2, 2014

The *Annual Review of Analytical Chemistry* is online at anchem.annualreviews.org

This article's doi: 10.1146/annurev-anchem-071213-020323

Keywords

single-cell proteomics, microfluidics, immunoassays, protein signaling

Abstract

We review an emerging microfluidics-based toolkit for single-cell functional proteomics. Functional proteins include, but are not limited to, the secreted signaling proteins that can reflect the biological behaviors of immune cells or the intracellular phosphoproteins associated with growth factor–stimulated signaling networks. Advantages of the microfluidics platforms are multiple. First, 20 or more functional proteins may be assayed simultaneously from statistical numbers of single cells. Second, cell behaviors (e.g., motility) may be correlated with protein assays. Third, extensions to quantized cell populations can permit measurements of cell–cell interactions. Fourth, rare cells can be functionally identified and then separated for further analysis or culturing. Finally, certain assay types can provide a conduit between biology and the physicochemical laws. We discuss the history and challenges of the field then review design concepts and uses of the microchip platforms that have been reported, with an eye toward biomedical applications. We then look to the future of the field.

1. INTRODUCTION

Over the past 25 years, microfluidic techniques (1) have emerged for the manipulation, sorting, and analysis of small biological samples, ranging from microliters of blood (2) to single cells (3, 4). On-chip assays range from cell counting to molecular measurements, with applications that span broadly across the fields of biology and biomedicine. Many of these microchip tools have been extensively reviewed in the recent literature (5–11). One of the newer technologies to emerge, and to be adapted to microchip formats, is single-cell functional proteomics. Functional proteins include the secreted cytokines, chemokines, proteases, and granulocytes that are commonly associated with immune cell function (12) but are also observed for other cell types. Functional proteins also include catalytically active (e.g., phosphorylated) kinases and associated effector proteins. This protein class comprises the intracellular signaling cascades (13), which are often hyperactivated in cancer cells and are consequently targeted by anticancer therapies (14). In their active states, such proteins have functional consequences that can be associated with the various hallmarks of cancer (15, 16). The kinetics, abundances, and statistical distributions of functional proteins often set them apart from their nonfunctional counterparts. Thus, we begin in Section 2 with a discussion on a few representative examples of functional proteins, with an eye toward identifying those practical issues associated with single-cell assays.

The first reports of microchip platforms for single-cell functional proteomics appeared just within the past decade (17–20). However, the technology has evolved rapidly such that several clinically relevant and uniquely enabled applications have been reported. This suggests that, in the near future, at least some of these platforms will emerge as clinical tools for helping guide patient care. This rapid advance is due, in large part, to the long history of single-cell proteomics, which originated with techniques such as enzyme-linked immunosorbent spot (ELISpot) (21) and a host of cytometry methods. These techniques, which continue to serve as the gold standard for most single-cell proteomics assays, have guided the development of microchip-based technologies and have defined many of the important biological problems for investigation. In Section 3, we discuss some of that history and how it has influenced the development of the microchip platforms that are the subject of this review.

Microchip platforms for single-cell functional proteomics are based on either staining and imaging fixed cells (22) or putting live cells into small environments such as microbubbles (18) or microchambers (17, 20) for analysis. Each of these tools has distinct advantages and disadvantages, and a few have advanced toward being applied to addressing biomedical or clinical problems. Such applications, which imply significant scientific and engineering demands, have, in fact, served as technology drivers. We list those demands here. (*a*) Clinical applications imply single-use microchips, and thus the chips must be inexpensive to fabricate in at least moderate throughput, and in a highly reproducible manner. (*b*) In single-cell biology, statistical numbers of single cells (hundreds to thousands) must be analyzed for any given assay to generate a meaningful result (23). (*c*) The proteomics (and other on-chip) assays must be robust and highly reproducible so that meaningful comparisons can be made between data sets collected across time points, patient samples, assay conditions, etc. (*d*) For many problems, the relevant functional proteins are present at low abundance (10^2–10^4 copies per cell). As a general rule, primary cells (direct from blood or tissue) contain significantly lower copy numbers of a given protein than do cultured cells. Thus, assay sensitivity is an important factor. Demands *a* and *b* largely describe engineering challenges, whereas demands *c* and *d* have mostly been addressed through a combination of surface chemistry approaches, coupled with advances in biomolecular labeling chemistries. In Section 4, we review the basic microfluidics platforms that have been reported. Because this is an analytical chemistry review, we emphasize quantitative measurement challenges

and the engineering and surface chemistry solutions that are permitting those challenges to be addressed.

In Section 5, we highlight applications in which microchip-based single-cell proteomics tools are providing unique and useful advantages. One major area has been in the design of platforms that integrate different assays, such as measurements of cell motility (24) or immune cell activation (25), correlated with functional proteomics assays from those same cells. A second area has been the ability to execute proteomics assays on quantized cell populations (i.e., 1, 2, 3. . .cells). These allow for a detailed analysis of specific cell–cell interactions (26, 27). A third area has been with regards to the numbers and types of functional proteins that can be assayed per cell, as well as the level of absolute quantitation and sensitivity that can be achieved (28). These capabilities open up new classes of systems for investigation. One such example involves the intracellular phosphoprotein signaling networks within cultured or primary cancer cells and the influence that targeted drugs can have on those networks (29, 30).

Finally, in Section 6, we look toward the future. Some of our projections are straightforward, such as anticipating the increase in technical capabilities of the microchip platforms, including the integration of multiple omic-type assays on the same single cells. An area that is less defined, but very important, involves the development of a discovery-based single-cell proteomics approach. All existing single-cell proteomic methods rely on antibodies and as such are targeted toward measuring the levels of specific proteins, the identities of which are predetermined. An approach that can go beyond this limitation, perhaps involving mass spectrometry (31), is a grand challenge of the field.

An area of single-cell functional proteomics that is omitted from this review is optical studies that utilize genetically modified cells as a means of generating in situ optical readouts of protein expression levels (see, e.g., 23, 32, 33). Such investigations are revealing a rich biology that is highly relevant to many of the basic concepts stressed here.

2. DETECTING FUNCTIONAL PROTEINS FROM SINGLE CELLS: RELEVANT PARAMETERS

Functional proteins are often transient and low-abundance targets for measurement. They are typically generated, released, and/or activated following stimulation, and their production is often the end result of a series of stochastic events. In other words, they are the opposite of housekeeping proteins (such as actin) that are present in abundant and reasonably stable concentrations. Thus, experimental designs for capturing functional protein levels from single cells should take into account several factors, including (*a*) the expected number of copies that are produced by individual cells; (*b*) the stimulation conditions required to generate such proteins; (*c*) the expected variance in protein number as measured across many single cells; and (*d*) the kinetics associated with that production, which can often compete with kinetics for the degradation of that same protein. Additional relevant factors include the cell type and cell phenotype, whether the cell is from culture or is a primary cell, and the history of the cell prior to analysis. Providing a comprehensive description of these factors is well beyond the scope of this review. However, it is instructive to consider a few illustrative examples, which are provided in **Table 1**. Listed in the table are three secreted proteins, including the cytokine tumor necrosis factor-α (TNF-α), the cytotoxic granule Granzyme B (GB), the secreted growth factor [vascular epithelial growth factor (VEGF)], a phosphorylated (p-) receptor tyrosine kinase (RTK) [epidermal growth factor receptor (EGFR)], and a cytoplasmic phosphokinase [p-extracellular signal-regulated kinase (ERK)].

The first entry is TNF-α, which, along with interferon-γ (IFN-γ), often provides a marker for immune cell activation. TNF-α is produced by numerous cell types following specific

Table 1 Descriptions and experimentally relevant parameters for selected functional proteins[a,b]

Protein	Description	Copy numbers per cell and basic quantitative description
TNF-α	This is a cytokine secreted by many (mostly immune) cell types (e.g., macrophages, T cells, and neurons) following cell stimulation. It is involved in systemic inflammation and stimulates acute phase reaction (109). TNFα is a drug target for certain autoimmune diseases.	It requires cell stimulation. Tumor antigen-specific $CD8^+$ T cells secrete from $<10^1$ to $>10^5$ copies over 12 h (**Figure 1**). A secretion rate of 10 copies sec^{-1} was measured from influenza antigen-specific $CD4^+$ T cells (25).
GB	This is a serine protease (enzyme) present in cytotoxic T lymphocyte and NK cell granules. Following cell stimulation, GB induces apoptosis in the target cell (110).	Commercial protein is not readily available, so an absolute calibration of assayed protein levels is not possible. Copy numbers secreted from tumor antigen-specific $CD8^+$ T cells over a 12-h period poststimulation span a range of 10^5 across individual cells (28).
p-EGFR	This is a cell surface RTK that is related to HER2/c-neu and other RTK drug targets. Stimulation by TGF-α or EGF phosphorylates EGFR. p-EGFR dimerizes and then activates signaling through many phosphoprotein pathways (111).	An average of 2×10^3 copies of phosphorylated wild-type EGFR per cell was present in model brain cancer cells containing the EGFR variant III oncogene (U87 EGFRvIII cells). The copy numbers range from 10^2 to near 10^5 (29). (See entry below for phosphorylation kinetics description.)
p-ERK	p-ERK is a cytoplasmic kinase that is also called classical MAPK. It is activated by growth factors, hormones, and other signals. Disruption of the ERK signaling pathway is common in cancers (14).	2,000–30,000 copies of p-ERK are produced by nonstimulated model brain cancer (U87) cells. Between 10,000–100,000 copies are present in those same cells following EGF stimulation (29). Phosphorylation occurs within 2–3 min of stimulation. In the absence of stimulation, phosphoprotein levels begin to decay within ~20 min.
VEGF	This is a secreted growth factor. It is an oncology and ophthalmology drug target (112).	Between 10^3 and 10^5 copies were secreted from model U87 EGFRvIII brain cancer cells over a 7-h period (30).

[a] See cited literature for the measurement details.

[b] Abbreviations: EGF(R), epidermal growth factor (receptor); ERK, extracellular signal-regulated kinase; GB, Granzyme B; HER2/c-neu, human epidermal growth factor receptor 2; MAPK, mitogen activated protein kinase; RTK, receptor tyrosine kinase; TGF, transforming growth factor; TNF, tumor necrosis factor; VEGF, vascular epithelial growth factor.

stimulations, so any single-cell assay should involve an activation step or be designed to probe otherwise activated cells. TNF-α can be produced in large copy numbers ($>10^6$ per cell within a 6-h period) and relatively quickly (10 per second). However, often only 10% of the total cell population will produce significant amounts of this protein. This low fraction of secretors may be associated with the relationship of the individual cells to their positions in the cell cycle (34), the stochastic nature of biology, the prior history of the cells, etc. The low fraction of protein-producing cells is just one of the many factors that illustrate the need to assay statistically significant numbers of cells. Such statistics are straightforward for flow cytometry but must be specifically designed into any microfluidics platform. **Figure 1** provides one-dimensional scatter plots showing how the average level and variance of a panel of secreted proteins, including TNF-α, differs among five immunotherapy cancer patients. These data were collected on a single-cell barcode chip (SCBC) (see Section 4) and illustrate the value of absolute calibrations. Those calibrations permit comparisons across different proteins and patients in this figure but also across time points, drug treatments, etc. Such calibrations are tough to do using flow cytometry. They rely on the availability of standard proteins and as such should also be interpreted with some caution. For example, proteins from a primary source may have different posttranslational modifications relative to the standard protein, and this can influence assay sensitivity.

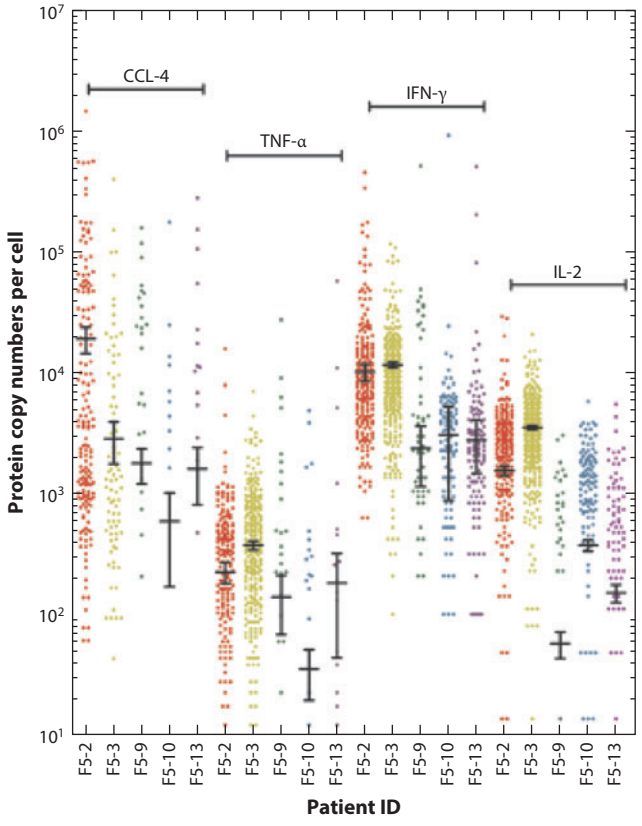

Figure 1

Scatter plots of the copy numbers per cell of three cytokines and CCL-4 assayed from single tumor antigen-specific $CD4^+$ and $CD8^+$ T cells collected from five cancer patients participating in an immunotherapy trial. Each dot is a single-cell assay. The measurement error is approximately 10%, and thus the distribution of protein levels reflects immune system heterogeneity which, for a given patient and by this metric, can span many orders of magnitude. Absolute calibrations were done with commercially available standard proteins. These data were collected and processed according to protocols outlined in Reference 28. Abbreviations: CCL, chemokine C-C motif ligand; CD, cluster of differentiation; IFN, interferon; TNF, tumor necrosis factor.

GB is secreted by certain immune cell phenotypes for cell killing functions. GB is not always commercially available (such is the case for many proteins), and this can preclude assay calibration. However, one can estimate the statistical variance of the abundance distribution across a relevant cell population if the immunoassay signal levels are in the linear regime. For a fluorescence assay, that is the range within a log-log plot of the measured fluorescence versus concentration that yields a straight line. The variance in protein abundance across many otherwise identical single cells will typically be high for almost any functional protein (**Figure 1**), but the details of that variance, and how it changes in response to some perturbation, contains biological information (see Section 5). For a protein such as GB, most activated cells will not secrete GB at levels much above baseline, but the cells that are active secretors can be extremely active—effectively producing a bimodal population of secretors and nonsecretors.

The third protein in **Table 1** is an activated (phosphorylated) membrane receptor kinase, p-EGFR, and the fourth is an activated cytoplasmic phosphokinase, p-ERK. Such kinases can

typically be phosphorylated at any number of sites—not all of which significantly increase enzyme activity. Monoclonal antibodies that exhibit avidity for specific phosphorylated residues of specific proteins are used for detecting activated (and thus functional) kinases in both single-cell and bulk assays. The average number of copies of p-EGFR per cell (for model brain cancer cells) is approximately 2,000. Of course, if the cells are fixed, made permeable, and then antibody-stained for the presence of these proteins, 2,000 copies within a single cell is a relatively high concentration (micromolar order) (22, 35, 36). However, if the cell contents are spilled out into microchambers with volumes in the 0.1–1-nL range, 2,000 protein copies translates into a 3–30-picoM concentration, which can push the limits of many fluorescent enzyme-linked immunosorbent assays (ELISAs). This highlights the need for strict attention to assay conditions. It isn't just about the antibodies! Surface chemistry also plays important roles. Phosphoproteins, such as p-EGFR and p-ERK, can be parts of the same intracellular signaling network. For example, activation of EGFR (to form p-EGFR) can, in turn, lead to ERK phosphorylation. Thus, ERK is called a downstream effector of EGFR. The implication is that the abundance of p-ERK within a cell will be positively influenced by the abundance of p-EGFR. Quantifying such protein relationships is an important piece of what is captured in a multiplexed single-cell functional proteomics assay.

The last protein, VEGF, is a secreted growth factor and a ligand for the VEGF receptor (VEGFR). It is associated with normal tissue function, but it is also associated with promoting angiogenesis in many solid tumors. From a detection standpoint, VEGF is similar to TNF-α, although, in hypoxic tumors, its production is often associated with the transcription factor hypoxia inducible factor (37). Thus, for certain single-cell studies, it may be desirable to simultaneously monitor VEGF secretion levels and phosphoprotein signaling pathways. This highlights the interesting challenge of monitoring multiple classes of proteins (secreted, cytoplasmic, membrane) from the same single cells.

3. HISTORY OF NON-MICROCHIP SINGLE-CELL PROTEOMICS TOOLS

Single-cell proteomics methods have evolved over more than 50 years, dating back to the invention of the Coulter counter (38), which evolved into the first cytometers (39). The emergence of lasers, photon detectors, high-speed electronics, bioconjugation chemistries, and dye molecules fed into the development of fluorescence flow cytometry (FFC) (40), fluorescence-activated cell sorting (FACS) (41), and ELISpot (21). Most recently, mass spectrometry advances have been harnessed for the development of mass cytometry (42). Excepting ELISpot, the dominant applications of these tools have been for sorting or enumerating cellular phenotypes based on measurements of surface marker (membrane) proteins. Intracellular staining (ICS) techniques have opened FFC and mass cytometry up to the analysis of at least a few cytoplasmic functional proteins per cell. Each of these techniques has strongly influenced the development and/or the specific applications of the more recent microchip tools.

3.1. The Enzyme-Linked Immunosorbent Spot Method

ELISpot intrinsically assays for functional proteins (43). The cells of interest (typically immune cells) are localized on a plate using surface-bound capture antibodies against specific cell surface markers. That surface is also coated with capture antibodies against specific secreted proteins. When the bound cells secrete proteins, fluorophore-labeled secondary antibodies are employed to bind to those captured proteins and provide a readout. By spatially correlating fluorescent spots with the locations of attached cells, the fraction of cells that are active secretors is recorded.

ELISpot assays are colorimetrically limited to the detection of approximately three proteins, but even with this limitation, ELISpot assays have been broadly used for monitoring immune system activation, most commonly by monitoring IFN-γ release (see, e.g., 44, 45). However, other functions, such as cell-mediated cytotoxicity, can be tracked via ELISpot assays of GB and other cytotoxic granules (46). ELISpot assays have provided several important lessons. First, secreted proteins from single cells may be readily detected with standard, sandwich-type ELISAs (47, 48). Second, well-defined immune cell phenotypes can be functionally heterogeneous. Third, ELISpot assays begin to hint at the importance of immune cell function, relative to immune cell population abundance, in terms of understanding various disease processes.

3.2. Multicolor Fluorescence Flow Cytometry, Fluorescence-Activated Cell Sorting, and Mass Cytometry

FFC and FACS are the dominant workhorses for single-cell proteomics. They bring a reasonably high level of multiplexing. Measurements of 6–10 simultaneous parameters per cell are practical, and analysis of up to 19 or so parameters is possible with highly specialized equipment (49). In this parlance, two parameters are associated with light scatter (forward and side) for discriminating between broadly different cell types (e.g., monocytes and platelets). The rest of the parameters are colorimetric, typically associated with different membrane proteins that are assayed using fluorophore-labeled antibodies. A triumph of modern biology has been the identification of cell surface markers that allow, by FACS, the enumeration and sorting of specific cellular phenotypes from blood or tissues. For example, a cytotoxic T cell is defined by the cell surface markers cluster of differentiation (CD)3, CD45, and CD8, with additional markers specifying the antigen specificity of the T-cell receptor (TCR) or providing further phenotypic classification, such as effector memory (50). Mass cytometry, which was recently developed by Nolan's (42) group, extends the concept of FFC to a substantially higher level of multiplexing through the use of antibodies that are tagged with mass labels, rather than fluorophore labels. Measurements of up to 34 parameters at the single-cell level (binding of 31 antibodies, cell viability, DNA content, and relative cell size) (42) have been reported. The power of flow cytometry tools to sort specific cell types and to even help define immune cell differentiation (42, 49–51) has strongly influenced our basic picture of the immune system and how it functions in response to specific threats. Not coincidentally, immune cell biology has provided an important scientific driver for the development of microchip-based single-cell proteomics.

Protein cell surface markers permit the sorting of cellular phenotypes from broad populations, but analyzing the functional performance of those phenotypes requires assays of functional proteins. For immune cell functions, these are normally secreted proteins that mediate the tasks of target killing (GB), self-renewal [interleukin (IL)-2 for T cells], recruitment of other immune cell types, inflammation (IL-6), and immune system regulation (IL-10), etc. The relative levels of a few (typically two to five) of these proteins may be monitored through the use of ICS FFC (52, 53). ICS FFC involves first blocking protein secretion and then fixing and making permeable the cells to allow for perfusion of antibody-labeled dyes. Although the blocking of protein secretion is a significant perturbation, much has been learned using ICS FFC. Examples include an understanding of the influence of pathogens toward steering functional diversity in phenotypically defined populations, as well as the importance of the specific nature of that functional diversity in immune responses to specific threats. Using similar cell staining protocols (54, 55), ICS FFC has also been utilized to investigate the structure of phosphoprotein signaling pathways (36, 56, 57). Those studies, which are almost exclusively from Nolan's (42) group, have been limited in number but highly informative. This highlights both the importance and difficulty of such investigations (58).

Again, flow cytometry methods have helped define the opportunity for using single-cell functional proteomics to elucidate phosphoprotein signaling pathways, and this has influenced applications in corresponding microchip tools.

4. MICROCHIP-BASED SINGLE-CELL PROTEOMICS METHODS

These tools use either antibody staining of the investigated cells (similar to flow cytometry or ICS FFC) or surface-based immunoassays (similar to ELISpot) to measure proteins released from the cells. Within these two primary classes, there are further differentiators; some tools permit control over the chemical environment around each of the assayed cells, whereas others analyze cells that are physically, but not chemically, isolated. This is an important distinction, because control over the chemical environment surrounding a cell can yield a screening tool. Almost all of the tools permit the cells to be visualized using microscopy, and so certain parameters, such as cell size and cell morphology, are basically a given.

4.1. Tools Using Cellular Staining Assays

Early generation microfluidics-based single-cell proteomics platforms were essentially miniaturized versions of FACS tools. For example, Quake's (59) group developed a micro(μ)-FACS chip for separating green-fluorescent protein-expressing *Escherichia coli* cells from a mixed population of nonfluorescent and fluorescent bacteria. The design used programmable flow conditions to switch flow directions and permit the cell types to be directed into different collection chambers. An enabling conceptual advance was the earlier development of integrated microfluidics platforms that incorporated valves, mixers, microchannels, and microchambers onto the same microchip (1). This design flexibility has been adapted for some of the recent microchip proteomics platforms and has also been important in the development of tools for single-cell transcriptome analysis (3). Other variations have emulated the concepts of ICS FFC. Sun et al. (22) utilized multicolor analysis of fluorescent antibody-labeled cytoplasmic proteins to assay for six parameters from single cells (binding of four antibodies and cell size and DNA content) from several human brain tumor biopsies. Using fixed and permeable cells, they stained for the proteins EGFR, p-Akt (protein kinase B), p-S6k, and phosphatase and tensin homolog. These proteins are associated with the phosphoinositide 3-kinase/Akt/mammalian target of rapamycin (mTOR) signaling pathway that is hyperactivated in many cancers, including many brain cancers. This type of analysis requires much smaller sample sizes than are needed for flow cytometry, and the microchip platforms are also relatively inexpensive. Gerdes et al. (60) reported on a sequential staining procedure of formalin-fixed, paraffin-embedded tissues that permitted a high level (~60 parameters) of multiplexing in what was effectively an advanced immunohistochemical staining approach that permitted some analysis at the single-cell level.

Virtually all other microfluidics single-cell proteomics tools utilizing cellular staining also separate the cells prior to analysis. One set of platforms, called cell arrays (19, 35, 61), uses arrays of micropatterned structures (microhurdles) to catch cells from a flowing single-cell suspension. The cells are physically separated, but not chemically isolated, from each other. Without chemical isolation, cell array assays yield information similar in nature to ELISpot assays, or even single parameter ICS FFC, in that the percentage of cells expressing a particular protein is measured (**Figure 1**). That (*a*) the chemical treatment to fix and perfuse cells with labeled antibodies is readily automated and quite rapid and that (*b*) very small numbers of cells are needed relative to an ICS FFC assay are inherent advantages to cell arrays. Eyer et al. (62) reported on a variation of cell arrays in which cells were captured in the types of microhurdles shown in **Figure 1*a*,*b***; however, the

design permitted additional control over the chemical environment of the cells, although it did not allow for such control at the single-cell level. Those workers developed a fluorescent readout assay for detecting the enzyme NAD(P)H oxidase from single cells, and applied it toward measurements of single-cell enzyme kinetics for specific biomolecular processes. Cell array experiments typically allow on the order of 10^2 single-cell assays.

Microdroplets (63) provide a related approach but one that permits control over the microenvironment surrounding each cell (18). To date, there is not much literature in this area, although, with additional development, the concept might evolve into a viable screening approach. Control over the local chemical environment surrounding each cell is a distinguishing characteristic, because it can permit experiments that are hard to envision with flow cytometry or ELISpot. Microdroplets also permit assays on quantized cell populations and, through calibration with fluorescently labeled beads, microdroplet immunoassays can yield absolute quantitation of protein copy numbers (64). Such calibrated assays, however, have not been applied to single cells but only to very small volumes of cell lysate.

4.1.1. Cell staining platforms: looking to the future. Those microchip platforms that rely on cell staining typically assay for one or two proteins per cell, although this limitation is not fundamental. Multicolor excitation and imaging techniques, coupled with modern dyes, should permit higher levels of multiplexing; however, they would also add much of the expense and sophistication of multicolor FFC but without the benefit of cell sorting. A more attractive option might be to use the imaging access afforded by these microchip tools to integrate super resolution imaging (65) with a conceptual extension of optical barcodes (66). For the barcoding, an antibody would be labeled with a long ssDNA oligomer. That DNA, in turn, is hybridized with short-chain, complementary ssDNA oligomers to which dyes are attached. Super resolution imaging can permit the spatial resolution of dye labels. Thus, with n colors and p dye positions, one can generate sufficient barcodes to detect n^p different proteins. This concept could rapidly yield multiplexing numbers that approach the size of the proteome. Although such an experiment is not currently practical, it provides at least a starting point for discussions regarding meeting the grand challenge of measuring the entire proteome within a single cell.

4.2. Tools Using Surface-Based Immunoassays

Tools using surface-based immunoassays are conceptually similar to ELISpot but have capabilities that can in many ways surpass those of cytometry tools. Separating protein assays from the cell implies that individual proteins can be spatially, rather than colorimetrically, identified, and that sandwich ELISA-type assays can be used. Of course, cell staining of proteins still can be simultaneously carried out. The result is a significantly higher level of multiplexing and, for some proteins, absolute quantitation. Second, intracellular, membrane, and secreted proteins may be assayed from the same single cell. Third, the chambers in which the cells are isolated can potentially accommodate multiple cells and/or cell types, thus permitting measurements of cellular interactions. Finally, these platforms allow the integration of functional assays (e.g., cell motility) with protein assays. In this class of platforms, only two base technologies—the microengraving technique from Love's group and our own SCBCs—have been reported, but both have been widely applied. We discuss the microengraving platforms first.

4.2.1. Microengraved single-cell proteomics chips. **Figure 2** employs an array of nearly 10^5 microwells to isolate and culture single cells and quantized cell populations. A microengraved (antibody-coated) substrate is used to cap the microwell array and to capture secreted proteins.

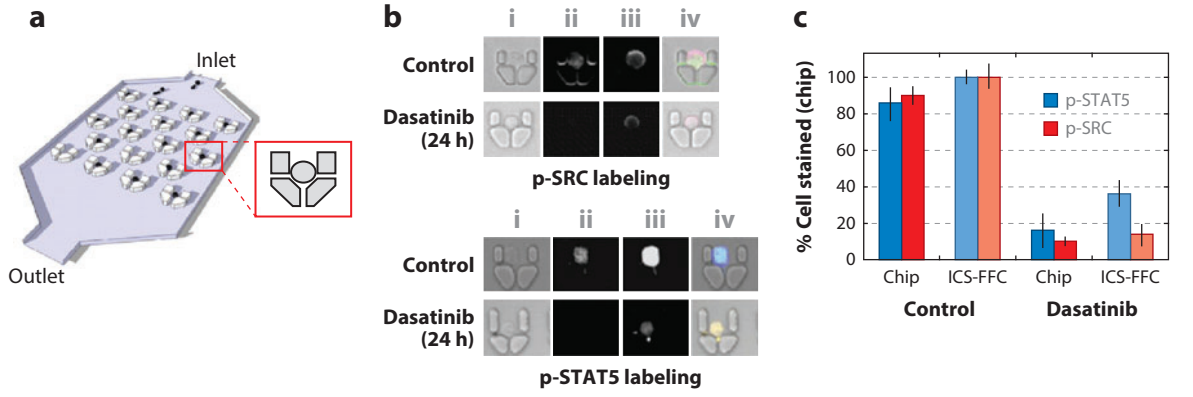

Figure 2

Cell array device applied for the rapid fixing and treatment of cells for staining intracellular phosphoproteins, applied here to illustrate the influence of the BCR/Abl and SRC tyrosine kinase inhibitor Dasatinib on patient-derived $CD34^+$ stem cells. (*a*) The cell array device. A single-cell suspension is introduced at the inlet, in which individual cells are trapped by specially designed microhurdles that permit liquid reagents to flow through. Once trapped, the cells can be rapidly fixed, permeabilized, and stained with phosphospecific antibodies. (*b*) Patient-derived stem cells pretreated with Dasatinib and then stained for the functional proteins p-SRC (*top*) and p-STAT5 (*bottom*), with and without Dasatinib treatment. The individual panels represent (*i*) bright field, (*ii*) fluorophore-conjugated anti-p-SRC (or p-STAT5) IgG, (*iii*) Annexin-V-Cy5 (*top*) or Sytox green (*bottom*), and (*iv*) merged images. (*c*) Statistical comparisons between the on-chip assays and analogous assays using ICS-FFC. Figure adapted from Reference 35. Abbreviations: FFC, fluorescence flow cytometry; ICS, intracellular staining; STAT, signal transducer and activator of transcription.

Those proteins are assayed using sandwich ELISAs, and up to three secreted proteins are simultaneously detected using colorimetric discrimination. Thus, the approach is similar to ELISpot but with a few important distinctions. Much higher statistics are achievable, the cells are chemically isolated, and the microengraved substrate can be replaced in situ. Replaceable substrates enable single-cell kinetic studies (67). Substrate removal also allows access to specific cells, identified from the proteomics assays, for subsequent analysis or culture formation (68). Both of these advantages are very hard to replicate using flow cytometry tools. An additional advantage of the microengraving platform is that it can be modified for PCR-based detection of a few transcripts at the single-cell level (69), although the combination of proteins and transcripts from the same single cells, using microengraved platforms, has not yet been reported. **Figure 3** illustrates a microengraving experiment designed to detect antibody-secreting B cells collected from specific locations from a healthy mouse or a mouse model of the autoimmune disorder known as Sjögren's syndrome (68). B cells are analyzed, using the microengraved slide, for their production of antibodies and for the specificity of those antibodies against specific antigens. If certain of the B cells exhibit particularly interesting behavior, they can be recovered for further culture or analysis.

4.2.2. Single-cell barcode chips. SCBCs are versatile and information-rich tools in which single cells, or defined numbers of cells, are isolated within microchambers that each contain a many-element antibody array (the barcode). A few hundred to 10^4 individual microchambers are included within a single microchip. Depending on the application, microchamber volumes are between 0.1 and 2 nL (26, 28), and microchamber design and operation protocols can permit sandwich-type ELISA immunoassays of cytoplasmic, secreted, or membrane proteins with a measurement error of ~10% for a given protein level (29).

Standard protocols may be used for microchip construction, but the patterning approach for the antibody barcode has unique constraints. The barcode is the enabling SCBC technology;

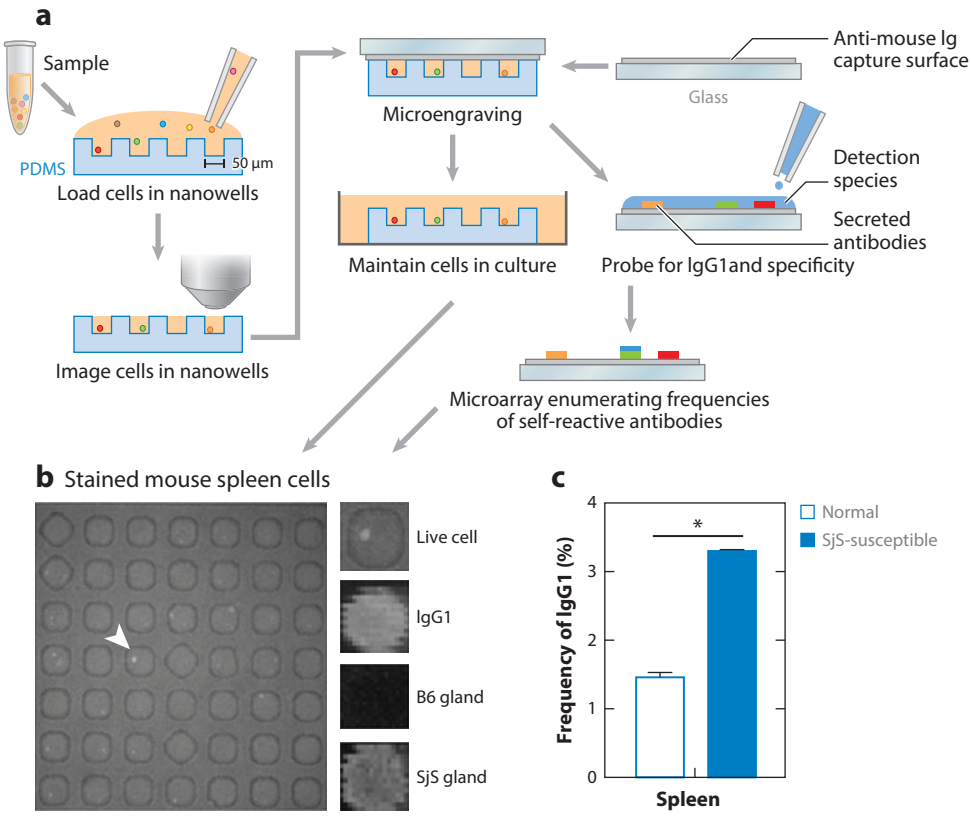

Figure 3

A microengraving experiment designed to capture and characterize antibody-secreting B cells reacting against salivary gland tissues in SjS (an autoimmune disease). (*a*) Process flow of experiment. (*b*) Micrograph of a portion of a nanowell array and microengraving assay results for the indicated microwell containing a single B cell. The cells are stained with calcein (live cells), FITC-dye-labeled CD19 and Cy7-dye-labeled CD4. The data presented for the live cell indicate production of antibodies that exhibit reactivity against SjS gland antigens. (*c*) Statistical analysis of the percentage of IgG1 producing B cells for both normal and SjS-susceptible mouse models. Adapted from Reference 68. Abbreviations: FITC, fluorescein isothiocyanate; PDMS, polydimethylsiloxane; SjS, Sjögren's syndrome.

as such, we discuss it in some detail here. Because of the instability of antibodies for long-term storage, or toward microchip processing conditions, the barcodes are initially patterned as ssDNA barcodes, with each barcode stripe having a unique ssDNA label. A cocktail of antibodies labeled with complementary ssDNA′ oligomers is used to convert the DNA barcode into an antibody barcode, just prior to running an assay (70–72). The microchamber surface area available for a typical 20-element barcode is between 150 × 150 μm^2 and 1,000 × 150 μm^2, implying each array element needs to be approximately 10–20 μm wide, at a 20–40-μm pitch. Such dimensions may be read with a standard array scanner (73) but are beyond the resolution of standard spotting tools (74). Molecular patterning tools that can approach these dimensions include molded elastomer stamping (75, 76), dip pen lithography (77), and microfluidic flow patterning (78). Of these choices, stamping does not permit the required level of multiplexing, whereas dip pen does not yield a surface coverage sufficient for stable and sensitive assays. Thus, we have developed microfluidic

flow patterning into the method of choice for SCBCs, including even building robotics systems to automate the task (79). In **Figure 4** we provide data showing the influence of various barcoding surface chemistries on assay sensitivity, some of which are described in Reference 20. Details of the ssDNA oligomers and antibody pairs used in SCBCs can be found in the supplementary materials of numerous publications (2, 28, 30, 80). The flow patterning approach described in **Figure 4** can be modified for doubling the density of the antibody arrays (26, 81).

Figure 5 depicts an SCBC microchamber designed for assaying phosphoprotein signaling pathways from single cells, along with representative data from such an assay. A full SCBC data set may contain 20 or more assayed proteins (R. Fan, unpublished data) and is recorded as a table. Each row corresponds to a microchamber address, and the columns contain the numbers and locations (or other descriptors) of cells within that microchamber, as well as the assayed levels of the individual proteins.

5. BIOLOGICAL AND BIOMEDICAL APPLICATIONS

5.1. Immunology and Immune Monitoring

Because of the variety of potential pathogen targets, cellular immunity is functionally heterogeneous, which is a characteristic uniquely quantitated at the single-cell level. Many efforts to capture this heterogeneity have used ICS FFC. An example is the work of Betts et al. (82), who measured five functions (degranulation and levels of IFN-γ, macrophage inflammatory protein 1b, TNF-α, and IL-2) from single HIV-specific $CD8^+$ T cells collected from chronically HIV-infected individuals and showed that the number functions (the polyfunctionality) were inversely correlated with viral load in those patients. Newell et al. (51) used ICS mass cytometry to assay 17 membrane protein markers, 6 intracellular cytokines, and 2 cytotoxic granules from stimulated $CD8^+$ T cells from healthy patients. They found an almost combinatorial distribution of cytokine secretion profiles across the individual cells, but there were distinct niches occupied by virus specific cells.

Microfluidic platforms have also been used to address the question of functional heterogeneity in cellular immunity. Ma and coworkers (28, 80) reported on the longitudinal monitoring of patients undergoing TCR-engineered adoptive cell transfer (ACT) cancer therapy (83). This cell-based immunotherapy was for the treatment of metastatic melanoma. SCBCs were used to compare the functional diversity of tumor antigen (MART-1)-specific $CD8^+$ T cells collected from the blood of melanoma cancer patients with $CD8^+$ T cells collected from healthy donors. They combined 19-plex SCBC functional (secreted) protein assays with 10-color FACS to measure the functional evolution of specific T-cell phenotypes at 5 to 10 time points over a 90-day trial. These measurements led to several conclusions. First, for a given patient and T-cell phenotype, if all single-cell data from all time points were coanalyzed, a level of functional coordination was resolved, meaning that the T cells could be loosely classified according to biological behaviors, such as antitumor or proinflammatory behaviors. Second, the most polyfunctional cells dominated the immune response: Roughly 10% of the cells of a given phenotype secreted five or more different proteins and, for any one of those proteins, those highly functional cells secreted, on average, 100-fold more protein copies than the less polyfunctional cells. Thus, for a given phenotype, 10% of the cells dominated the overall immune response by tenfold. This led to the defining of a polyfunctionality strength index. Interestingly, although the cellular population dynamics or phenotype changes (such as naïve or central memory) over the course of the trial did not yield clear clinical correlates, the polyfunctionality kinetics did correlate with clinical observations, providing feedback for potentially improving the ACT trial design. This collective work over the

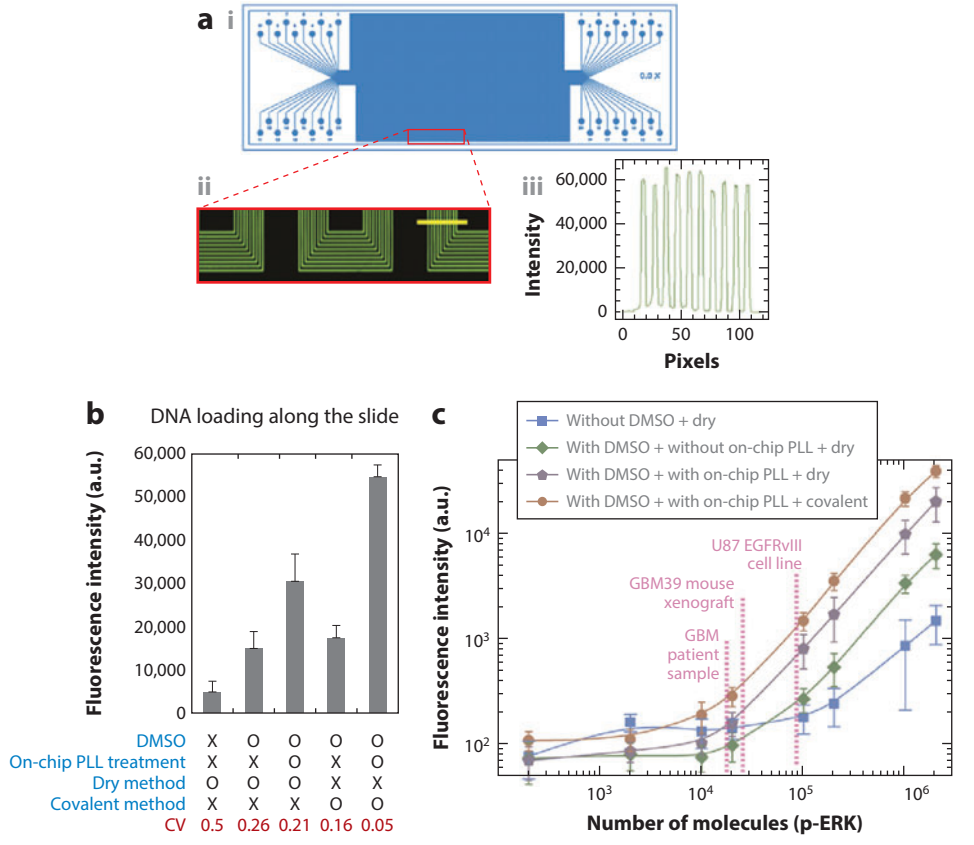

Figure 4

The surface chemistry of DNA barcode patterning and its importance for quantitative single-cell protein immunoassays. (*a*) The microfluidic flow patterning template used to prepare barcodes on PLL-coated glass slides. (*i*) The elastomer flow patterning mold contains one channel for each barcode stripe, and a mold for a 20-element barcode is drawn. The channels meander across the glass surface and are on the order of 1 m long and 10–20 μm wide, depending on the design. (*ii*) ssDNA oligomers are initially patterned, and the quality of those DNA barcodes is assessed by hybridizing each strand with a complementary, dye-labeled ssDNA′ oligomer. (*iii*) The digitized fluorescence micrograph shows the uniformity of a 10-element barcode across the region indicated by the yellow bar in *ii*. (*b*) Digitized fluorescence data reflect the DNA loading of 20-μm-wide barcode stripes, based on various patterning chemistries. O means that the indicated chemistry was used, and X means that it was not used. CV values reflect the loading uniformity of the various patterning strategies. Surface chemistry definitions for panel *b*: On-chip PLL treatment: 0.1% PLL solution in PBS flows through the microchannels before DNA loading to increase the amount of amine groups that are used to immobilize DNAs. Dry method: After the channels are filled with DNA solution, the device is fully dried within a desiccator. The surface-adsorbed ssDNAs are cross-linked by thermal treatment (at 80°C for 4 h). Covalent method: A linker molecule that contains an amine-reactive NHS ester at each end of an eight-carbon spacer arm is used to immobilize amine-terminated DNAs to the PLL surface. (*c*) Calibration data for the protein p-ERK, measured using the various chemistries. Surface chemistry improvements yield more than a tenfold increase in assay sensitivity, enabling single-cell assays of both highly challenging primary tumor cells (the GBM patient sample) and model cell lines. Some of these data follow protocols outlined in Reference 20. Abbreviations: CV, coefficient of variation; ERK, extracellular signal-regulated kinase; GBM, glioblastoma multiforme; NHS, *N*-hydroxysulfosuccinimide; PBS, phosphate buffered saline; PLL, polylysine.

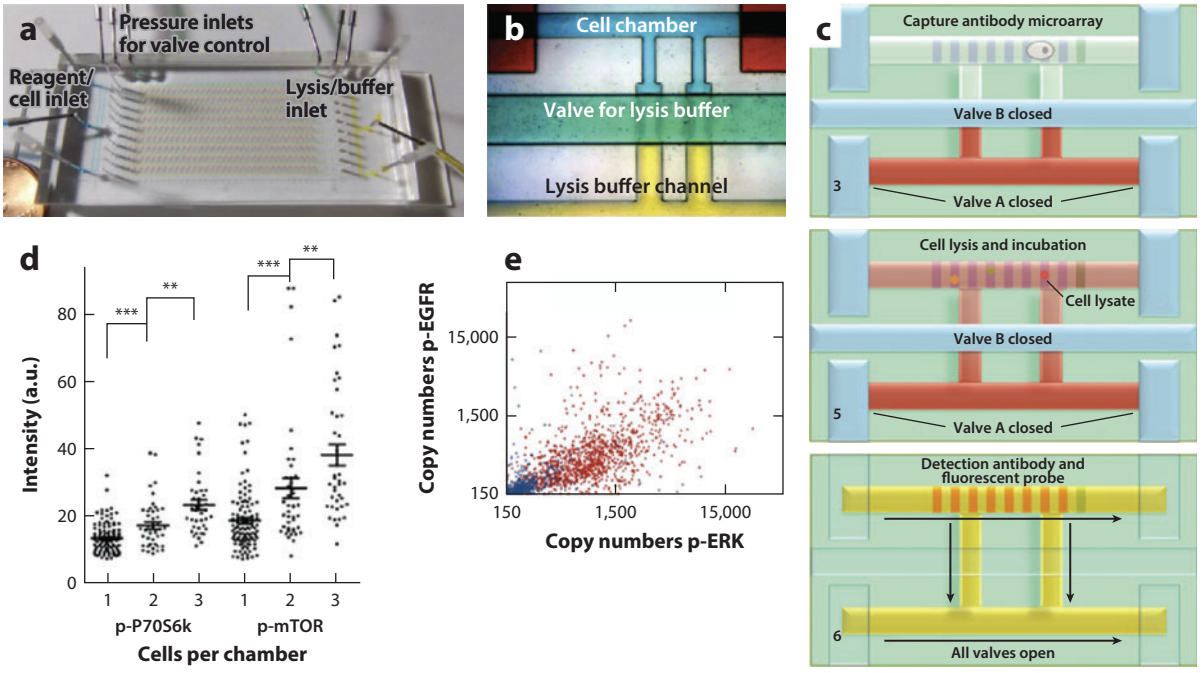

Figure 5

SCBC images, assay process flow, and representative data for assaying a panel of phosphoproteins from single cells. (*a*) A photograph of a 320-microchamber chip (a penny at bottom left provides scale) and (*b*) a higher resolution image of a single microchamber from that chip. The functional regions are colored with food dyes. (*c*) Process flow for capturing intracellular proteins. Cells are loaded onto the chip in the upper halves of the microchambers, and lysate buffer, with phosphatase and protease inhibitors, is loaded into the bottom halves. For assaying secreted proteins, the cells are incubated on-chip for a few hours. Otherwise, the microchip is cooled to 0°C, and valve B is opened for 30 min to diffuse lysis buffer into the upper chamber. The valve is closed, and the microchip is kept at room temperature for 2 h to permit capture of the released proteins. The SCBC is then flushed, and a cocktail of detection antibodies and fluorescent probes is introduced to develop the barcodes. The SCBC is disassembled to permit digitization of the barcode fluorescence using an array scanner. (*d*) Scatter plots of one-, two-, and three-cell protein assays of p-P70S6k and p-mTOR, as measured from the model GBM cell line U87EGFRvIII. Each dot is a single experiment, and the y-axis shows fluorescence intensities collected from a digitized barcode. The increase in average signal level (*black bars*) as the numbers of cells increase indicates that the measured protein abundances likely lie just below the linear response regime of the ELISA. (*e*) A scatter plot showing the correlation between two assayed proteins. Each dot represents a single experiment; red dots represent one-cell data and blue dots zero-cell data (background). Panel *e* is adapted from Reference 26; panels *a–d* are adapted from Reference 30. Abbreviations: ELISA, enzyme-linked immunosorbent assays; ERK, extracellular signal-regulated kinase; GBM, glioblastoma multiforme; SCBC, single-cell barcode chip.

past decade has refined the notion that the quality of a T-cell immune response is best captured by the functional performance of the T cells, rather than by their quantity (84).

Most reported applications of the microengraving platform have also focused on immunology (25, 67, 85–89). These investigations have emphasized types of experiments that are not tractable using the various cytometry methods. The first is the ability to replace, in situ, the microengraved slide that contains the immunoassays, thus permitting investigations of the kinetics of protein secretion (67, 89) from single activated T cells. Those studies resolve individual T cell secretion trajectories and have provided a higher resolution picture of T cell kinetics than can be captured by more traditional means (34, 90). A second aspect of the microengraving studies has been to identify immune cells with interesting functional properties and then find ways to separate those

cells for additional investigations (68, 88). Those studies are particularly interesting from the point of view of identifying antigen-specific cells (e.g., B cells or T cells). Such cells, although often difficult to isolate, play important roles in immune responses (91) or in therapies that rely on encouraging or engineering (92) such responses against disease-specific antigens. The microengraving platform may provide a viable approach toward identifying and characterizing these rare cells.

5.2. Phosphoprotein Signaling Pathways

For many cancers, genomic surveys are revealing a landscape of altered signal transduction cascades that often cluster along a set of druggable core pathways. In fact, these pathways contain molecular targets for newer generations of cancer therapies (14). However, the translation of genomic data into effective clinical treatments has been confounded because nongenetic cell-to-cell variability is profound in drug responses and resistance development. A recent editorial (93, p. 2) has pointed out that capturing the functional protein signaling networks may prove valuable for this purpose, because those signaling proteins, "not the genes per se, are responsible for the phenotypes of tumors and for the emergence of therapeutic resistance." Single-cell proteomics provides the most direct approach for elucidating protein signaling network structure and coordination, and information from such measurements emerges at many levels. First, the spread (variance) in copy numbers of a given protein, as measured across each of many otherwise identical single cells (see **Figure 1** or **Figure 5*d***), can represent the functional heterogeneity of that protein. Population heterogeneity can arise from factors such as the stochastic nature of intracellular events (94) controlled by low-copy-number transcription factors (95) or through cell–cell interactions (95, 96). The net result may be high-amplitude fluctuations at the single-cell level but stability across a population (97). In other words, the population is stable exactly because it is heterogeneous (consider, for example, the robust nature of a diverse economy). This concept can be quantified using statistical physics models. Thus, fluctuation measurements can capture cellular heterogeneity, while simultaneously providing a measure of the stability of the organelle, tumor, etc., that is comprised of those cells and providing a bridge to statistical physics models with predictive capacity. This approach contrasts with traditional biology thinking, which might seek to classify the population into functional phenotypes. Such thinking discards the heterogeneity of the system in favor of a more streamlined (but ultimately nonpredictive) description.

A second level of information involves protein–protein correlations (**Figure 5*e***). Correlations and anticorrelations can imply activating and inhibitory interactions. This means that measurements with higher multiplexing capacity will capture larger numbers of such interactions and thus increasingly resolve the associated protein signaling network (29, 57). The use of physicochemical laws to predict biological behaviors based on single-cell proteomics assays has been studied by Shin et al. (98) to investigate (and predict) how stimulated macrophage cells respond to various perturbations. More sophisticated, but related, approaches were applied to study the influence of hypoxia (reduced O_2 partial pressure) on glioblastoma multiforme tumors (30). For that study, highly specific and surprising predictions of hypoxia-dependent therapy resistance were made regarding the use of mTOR inhibitors to treat both cell lines and tumor models. Those predictions were verified.

Assays in which measurements of both cellular function and functional protein levels are executed from the same single cells represent experiments that are unique to the microchip platforms. Lu et al. (24), using a platform that was more or less an SCBC-microengraving hybrid, investigated a panel of 14 different secreted proteins, as well as motility assays, on model cancer cells, with

additional extensions to primary cells derived from patient brain tumors. They identified three specific secreted proteins that correlated with cell motility.

5.3. Cell–Cell Interactions

A unique aspect of microchip platforms is that they can permit investigations of quantized cell populations. Such explorations have focused, at varying levels of resolution, on the inhibitory or activating nature of intercellular interactions and have combined protein assays with functional observations (99–102). A recent study (26) correlated the levels of a panel of phospho- and secreted signaling proteins in model glioblastoma multiforme (brain cancer) cells, with cell–cell distances in two-cell assays. The work revealed that a detailed knowledge of pairwise cell interaction functions could be used to predict specific properties of larger cell populations. Such experiments again draw from concepts derived from statistical physics (103) and may eventually allow complex phenomena within tissue microenvironments to be understood.

Although not exactly single-cell work, Shao et al. (104) reported on protein typing of individual circulating microvesicles using a novel microchip/nuclear magnetic resonance system. Microvesicles (105) are significantly smaller than the cells that they originate from and can provide a medium for cell–cell communication (106) but may also provide a rich source of circulating tumor markers. This can be especially informative for intracranial tumors, which do not shed cells into the circulatory system.

Yamanaka et al. (27) utilized a microengraved platform to investigate the interactions between lymphocytes known as natural killer (NK) cells and target cells. NK cells can recognize and kill certain cells (such as viral infected cells) without the need for antigen recognition. The workers found that NK cells operate independently and promptly when lysing a single target cell. They also found that IFN-γ secretion correlates with low motility for NK cells that have contacted a target cell. These types of cell–cell interaction studies may eventually lead to an improved understanding of the functional heterogeneity of the immune system.

6. LOOKING TO THE FUTURE

Powerful tools such as mass cytometry have appeared over the past few years, but new classes of microchips for single-cell functional proteomics have also emerged with distinct and powerful advantages that are just now being explored. With such a rapidly developing field, looking into the future is tricky. One approach is to consider the low-hanging fruit, the technology bottlenecks, and the biological and clinical drivers that are pushing the field forward. For example, all the pieces currently exist to permit highly multiplexed transcriptome and proteome analyses of the same primary single cells; as such, this is a low-hanging fruit. The rapid advances of immunotherapy will likely push the development of such multilevel assays toward those that can identify and clone the very rare cells that produce particularly interesting antibodies or TCRs. Another clinical driver is the increase in the development and use of targeted cancer therapies, coupled with the confounding modest performance of those drugs that is often seen in the clinic. Bridging that gap will require resolving, at an unprecedented level, the structure of the phosphoprotein signaling networks that are targeted by those therapies.

A technical bottleneck involves the level of multiplexing achievable using current approaches. Both cytometry and microchip tools likely reach a limit between 50 and 100 proteins per cell. Even beating this limit by a factor of two or three would still represent sampling only a tiny part of the proteome. This limit arises because of the reliance on antibody-based detection schemes. Beating this limit will require either (*a*) a protein capture agent technology that is the equivalent

of very cheap, robust, and very high performing monoclonal antibodies or antibody-equivalents or (*b*) a discovery approach, such as mass spectrometry, for single-cell proteomics.

Finally, an increased emphasis on accurate and quantitative measurements will clearly push the field forward, simply because of the transportability of such measurements for comparisons across cell lines, patient samples, etc. This is a lesson drawn from the current revolution in mass spectrometry proteomics. Focused proteomics tools such as multiple reaction monitoring (107), coupled with the existence of the human peptide atlas (108), have brought mass spectrometry to the point where it is now being developed as a truly quantitative clinical diagnostics tool for measuring panels of protein biomarkers. The strong emphasis on quantitative and accurate measurements highlights the role of analytical chemistry for this field.

DISCLOSURE STATEMENT

The authors are not aware of any affiliations, memberships, funding, or financial holdings that might be perceived as affecting the objectivity of this review.

ACKNOWLEDGMENTS

A portion of the science described in this review was funded by the National Cancer Institute grants 5U54CA119347 and R01 CA170689-01, the Jean Perkins Foundation, and the Ben and Catherine Ivy Foundation.

LITERATURE CITED

1. Thorsen T, Maerkl SJ, Quake SR. 2002. Microfluidic large scale integration. *Science* 298:580–84
2. Fan R, Vermesh O, Srivastava A, Yen BKH, Qin L, et al. 2008. Integrated barcode chips for rapid, multiplexed analysis of proteins in microliter quantities of blood. *Nat. Biotechnol.* 26:1373–78
3. Ottesen EA, Hong JW, Quake SR, Leadbetter JR. 2006. Microfluidic digital PCR enables multigene analysis of individual environmental bacteria. *Science* 314:1464–67
4. Lorthongpanich C, Cheow LF, Balu S, Quake SR, Knowles BB, et al. 2013. Single-cell DNA-methylation analysis reveals epigenetic chimerism in preimplantation embryos. *Science* 341:1110–12
5. Heath JR, Davis ME. 2008. Nanotechnology and cancer. *Annu. Rev. Med.* 59:251–65
6. Toner M, Irimia D. 2005. Blood-on-a-chip. *Annu. Rev. Biomed. Eng.* 7:77–103
7. Zare RN, Kim S. 2010. Microfluidic platforms for single cell analysis. *Annu. Rev. Biomed. Eng.* 12:187–201
8. Choi K, Ng AHC, Fobel R, Wheeler AR. 2012. Digital microfluidics. *Annu. Rev. Anal. Chem.* 5:412–40
9. Han NH, Li CA, Seong GH. 2013. Microfluidic chips for immunoassays. *Annu. Rev. Anal. Chem.* 6:119–41
10. Wei W, Shin YS, Ma C, Wang J, Elitas M, et al. 2013. Microchip platforms for multiplex single-cell functional proteomics with applications to immunology and cancer research. *Genome Med.* 5:275–87
11. Wheeler AR, Throndset WR, Whelan RJ, Leach AM, Zare RN, et al. 2003. Microfluidic device for single cell analysis. *Anal. Chem.* 75:3581–86
12. Rawlings JS, Rosler KM, Harrison DA. 2004. The JAK/STAT signaling pathway. *J. Cell Sci.* 117:1281–83
13. Bhalla US, Iyengar R. 1999. Emergent properties of networks of biological signaling pathways. *Science* 283:381–87
14. Logue JS, Morrison DK. 2012. Complexity in the signaling network: insights from the use of targeted inhibitors in cancer therapy. *Genes Dev.* 26:641–50
15. Kroemer G, Pouyssegur J. 2008. Tumor cell metabolism: cancer's Achilles' heel. *Cancer Cell* 13:472–82
16. Hanahan D, Weinberg RA. 2000. The hallmarks of cancer. *Cell* 100:57–70
17. Love JC, Ronan JL, Grotenbreg GM, Van der Veen AG, Ploegh HL. 2006. A microengraving method for rapid selection of single cells producing antigen specific antibodies. *Nat. Biotechnol.* 24:703–7

18. Huebner A, Srisa-Art M, Holt D, Abell C, Hollfelder F, et al. 2007. Quantitative detection of protein expression in single cells using droplet microfluidics. *Chem. Commun.* 2:1218–20
19. Di Carlo D, Aghdam N, Lee LP. 2006. Single-cell enzyme concentrations, kinetics, and inhibition analysis using high-density hydrodynamic cell isolation arrays. *Anal. Chem.* 78:4925–30
20. Shin YS, Ahmad H, Shi Q, Kim H, Pascal TA, et al. 2010. Chemistries for patterning robust DNA microbarcodes enable multiplex assays of cytoplasm proteins from single cancer cells. *Chem. Phys. Chem.* 11:3063–306
21. Czerkinsky C, Nilsson L, Nygren H, Ouchterlony O, Tarkowski A. 1983. A solid-phase enzyme-linked immunospot (ELISPOT) assay for enumeration of specific antibody-secreting cells. *J. Immunol. Methods* 65(1–2):109–21
22. Sun J, Masterman-Smith MD, Graham NA, Jiao J, Mottahedeh J, et al. 2010. A microfluidic platform for systems pathology: multiparameter single-cell signaling measurements of clinical brain tumor specimens. *Cancer Res.* 70:6128–38
23. Welch CM, Elliott H, Danuser G, Hahn KM. 2010. Imaging the coordination of multiple signaling activities in living cells. *Nat. Rev. Mol. Cell Biol.* 12:749–56
24. Lu Y, Chen JJ, Mu L, Xue Q, Wu Y, et al. 2013. High-throughput secretomic analysis of single cells to assess functional cellular heterogeneity. *Anal. Chem.* 85:2548–56
25. Torres AJ, Contento RL, Gordo S, Wucherpfennig KW, Love CL. 2013. Functional single-cell analysis of T-cell activation by supported bilayer-tethered ligands on arrays of nanowells. *Lab Chip* 13:90–99
26. Wang J, Tham D, Wei W, Shin YS, Ma C, et al. 2012. Quantitating cell–cell interaction functions with applications to glioblastoma multiforme cancer cells. *Nano Lett.* 12:6101–6
27. Yamanaka YJ, Berger CT, Sips M, Cheney PC, Alter G, Love CJ. 2012. Single-cell analysis of the dynamics and functional outcomes of interactions between human natural killer cells and target cells. *Integr. Biol.* 4:1175–84
28. Ma C, Cheung AF, Chodon T, Koya RC, Wu Z, et al. 2013. Multifunctional T cell analyses to study response and progression in adoptive cell transfer immunotherapy. *Cancer Discov.* 3:418–29
29. Shi Q, Qin L, Wei W, Geng F, Fan R, et al. 2012. Single-cell proteomic chip for profiling intracellular signaling pathways in single tumor cells. *Proc. Natl. Acad. Sci. USA* 109:419–24
30. Wei W, Shi Q, Remacle F, Qin L, Shackelford D, et al. 2013. Hypoxia induces a phase transition within a kinase signaling network in cancer cells. *Proc. Natl. Acad. Sci. USA* 110:E1352–60
31. Angel TE, Aryal UK, Hengel SM, Baker ES, Kelly RT, et al. 2012. Mass spectrometry-based proteomics: existing capabilities and future directions. *Chem. Soc. Rev.* 41:3912–28
32. Spiller DG, Wood CD, Rand DA, White MRH. 2010. Measurement of single-cell dynamics. *Nature* 465:736–45
33. Taniguchi Y, Choi PJ, Li G-W, Chen H, Babu M, et al. 2010. Quantifying *E. coli* proteome and transcriptome with single-molecule sensitivity in single cells. *Science* 329:533–38
34. Bird JJ, Brown DR, Mullen AC, Moskowitz NH, Mahowald MA, et al. 1998. Helper T cell differentiation is controlled by the cell cycle. *Immunity* 9:229–37
35. Faley SL, Copland M, Reboud J, Cooper JM. 2011. Cell chip array for microfluidic proteomics enabling rapid in situ assessment of intracellular protein phosphorylation. *Biomicrofluidics* 5:024106
36. Gibbs KD Jr, Gilbert PM, Sachs K, Zhao F, Blau HM, et al. 2011. Single-cell phospho-specific flow cytometric analysis demonstrates biochemical and functional heterogeneity in human hematopoietic stem and progenitor compartments. *Blood* 117:4226–33
37. Dang CF, Kim J-w, Gao P, Yustein J. 2008. The interplay between MYC and HIF in cancer. *Nat. Rev. Cancer* 8:51–56
38. Coulter WH. 1953. Means for counting particles suspended in fluid. *US Patent No. 2,656,508*
39. Fulwyler MJ. 1965. Electronic separation of biological cells by volume. *Science* 150(698):910–11
40. Herzenberg LA, Parks D, Sahaf B, Perez O, Roederer M, Herzenberg LA. 2002. The history of the fluorescence activated cell sorter and flow cytometry: a view from Stanford. *Clin. Chem.* 48:1819–27
41. Herzenberg, LA, Julius MH, Masuda T. 1972. Demonstration that antigen-binding cells are precursors of antibody-producing cells after purification with a fluorescence-activated cell sorter. *Proc. Natl. Acad. Sci. USA* 69(7):1934–38

42. Bendall SC, Simonds EF, Qiu P, Amir ED, Krutzik PO, et al. 2011. Single-cell mass cytometry of differential immune and drug responses across a human hematopoietic continuum. *Science* 332:687–96
43. Moodie Z, Price L, Gouttefangeas C, Mander A, Janetzki S, et al. 2010. Response definition criteria for ELISPOT assays revisited. *Cancer Immunol. Immunother.* 59:1489–501
44. Hutchings PR, Cambridge G, Tite JP, Meager T, Cooke A. 1989. The detection and enumeration of cytokine-secreting cells in mice and man and the clinical application of these assays. *J. Immunol. Methods* 120:1–8
45. Banchereau J, Palucka AK, Dhodapkar M, Burkeholder S, Taquet N, et al. 2001. Immune and clinical responses in patients with metastatic melanoma to $CD34^+$ progenitor-derived dendritic cell vaccine. *Cancer Res.* 61:6451–58
46. Shafer-Weaver K, Sayers T, Strobl S, Derby E, Ulderich T, et al. 2003. The Granzyme B ELISPOT assay: an alternative to the ^{51}Cr-release assay for monitoring cell-mediated cytotoxicity. *J. Transl. Med.* 1:14
47. Engvall E, Perlman P. 1971. Enzyme-linked immunosorbent assay (ELISA). Quantitative assay of immunoglobulin G. *Immunochemistry* 8(9):871–74
48. Van Weemen BK, Schuurs AH. 1971. Immunoassay using antigen-enzyme conjugates. *FEBS Lett.* 15(3):232–36
49. Perfetto SP, Chattopadhyay PK, Roederer M. 2004. Seventeen-colour flow cytometry: unravelling the immune system. *Nat. Rev. Immunol.* 4:648–55
50. Altman JD, Moss PAH, Goulder PJR, Barouch DH, McHeyzer-Williams MG, et al. 1996. Phenotype analysis of antigen-specific T-lymphocytes. *Science* 274:94–96
51. Newell EW, Sigal N, Bendall SC, Nolan GP, Davis MM. 2012. Cytometry by time-of-flight shows combinatorial cytokine expression and virus-specific cell niches within a continuum of $CD8^+$ T cell phenotypes. *Immunity* 36:142–52
52. Sandberg JK, Fast NM, Nixon DF. 2001. Functional heterogeneity of cytokines and cytolytic effector molecules in human $CD8^+$ T lymphocytes. *J. Immunol.* 167:181–87
53. Lamoreaux L, Roederer M, Koup R. 2006. Intracellular cytokine optimization and standard operating procedure. *Nat. Protoc.* 1:1507–16
54. Krutzik PO, Nolan GP. 2003. Intracellular phospho-protein staining techniques for flow cytometry: monitoring single cell signaling events. *Cytometry* 55A:61–70
55. Krutzik PO, Irish JM, Nolan GP, Perez OD. 2004. Analysis of protein phosphorylation and cellular signaling events by flow cytometry: techniques and clinical applications. *Clin. Immunol.* 110:206–21
56. Irish JM, Hovland R, Krutzik PO, Perez OD, Bruserud O, et al. 2004. Single cell profiling of potentiated phospho-protein networks in cancer cells. *Cell* 118:217–28
57. Sachs K, Perez O, Pe'er D, Lauffenburger DA, Nolan GP. 2005. Causal protein-signaling networks derived from multiparameter single-cell data. *Science* 308:523–29
58. Altschuler SJ, Wu LF. 2011. Cellular heterogeneity: Do differences make a difference? *Cell* 141:559–63
59. Fu AY, Spence C, Scherer A, Arnold FH, Quake SR. 1999. A microfabricated fluorescence-activated cell sorter. *Nat. Biotechnol.* 17:1109–11
60. Gerdes MJ, Sevinsky CJ, Sood A, Adak S, Bello MO, et al. 2013. Highly multiplexed single-cell analysis of formalin-fixed, paraffin-embedded cancer tissue. *Proc. Natl. Acad. Sci. USA* 110:11982–87
61. Faley SL, Copland M, Wlodkowic D, Kolch W, Seale KT, et al. 2009. Microfluidic single cell arrays to interrogate signalling dynamics of individual, patient-derived hematopoietic stem cells. *Lab Chip* 9:2659–64
62. Eyer K, Kuhn P, Hanke C, Dittrich PS. 2012. A microchamber array for single cell isolation and analysis of intracellular biomolecules. *Lab Chip* 12:765–72
63. Theberge AB, Courtois F, Schaerli Y, Fischlechner M, Abell C, et al. 2010. Microdroplets in microfluidics: an evolving platform for discoveries in chemistry and biology. *Angew. Chem. Int. Ed.* 49:5846–68
64. Martino C, Zagnoni M, Sandison ME, Chanasakulniyom M, Pitt AR, Cooper JM. 2011. Intracellular protein determination using droplet-based immunoassays. *Anal. Chem.* 83:5361–68
65. Zhuang Z. 2009. Nano-imaging with STORM. *Nat. Photonics* 3:365–67
66. Cai L. 2013. Turning single cells into microarrays by super-resolution barcoding. *Briefings Funct. Genomics* 12:75–80

67. Varadarajan N, Julg B, Yamanaka YJ, Chen H, Ogunniyi AO, et al. 2011. A high-throughput single-cell analysis of human CD8$^+$ T cell functions reveals discordance for cytokine secretion and cytolysis. *J. Clin. Investig.* 121:4322–31
68. Nguyen CQ, Ogunniyi AO, Karabiyik A, Love CJ. 2013. Single-cell analysis reveals isotype-specific autoreactive B cell repertoires in Sjogren's syndrome. *PLoS One* 8:e58127
69. Gong Y, Ogunniyi AO, Love JC. 2010. Massively parallel detection of gene expression in single cells using subnanolitre wells. *Lab Chip* 10:2334–37
70. Niemeyer CM. 2005. Self-assembled bioconjugates for biochip technologies. *Int. J. Environ. Chem.* 85:639–43; Niemeyer CM. 2007. Functional devices from DNA and proteins. *Nano Today* 2:42–52
71. Bailey RC, Kwong GA, Radu CG, Witte ON, Heath JR. 2007. DNA-encoded antibody libraries: a unified platform for multiplexed cell sorting and detection of genes and proteins. *J. Am. Chem. Soc.* 129:1959–67
72. Boozer C, Ladd J, Chen SF, Jiang ST. 2006. DNA-directed protein immobilization for simultaneous detection of multiple analytes by surface plasmon resonance biosensor. *Anal. Chem.* 78:1515–19
73. Rose D. 2000. Microfluidic technologies and instrumentation for printing DNA microarrays. In *Microarray Biochip Technology*, ed. M. Schena, pp. 19–38. Walton-on-Thames, UK: Eaton
74. Barbulovic-Nad I, Lucente M, Sun Y, Zhang M, Wheeler AR, Bussman M. 2006. Bio-microarray fabrication techniques—a review. *Crit. Rev. Biotechnol.* 26:237–59
75. Xia YN, Whitesides GM. 1998. Soft lithography. *Angew. Chem. Int. Ed.* 37:550–75
76. Lange SA, Benes V, Kern DP, Horber JKH, Bernard A. 2004. Microcontact printing of DNA molecules. *Anal. Chem.* 76:1641–47
77. Lee K-B, Park S-J, Mirkin CA, Smith JC, Mrksich M. 2002. Protein nanoarrays generated by dip-pen nanolithography. *Science* 295:1702–5
78. Delamarche E, Bernard A, Schmid H, Michel B, Biebuyck H. 1997. Patterned delivery of immunoglobulins to surfaces using microfluidic networks. *Science* 276:779–81
79. Ahmad H, Sutherland A, Shin YS, Hwang K, Qin L, et al. 2011. A robotics platform for automated batch fabrication of high density, microfluidics-based DNA microarrays, with applications to single cell multiplex assays of functional proteins. *Rev. Sci. Inst.* 82:094301
80. Ma C, Fan R, Ahmad H, Shi Q, Comin-Anduix B, et al. 2011. A clinical microchip for evaluation of single immune cells reveals high functional heterogeneity in phenotypically similar T cells. *Nat. Med.* 17:738–43
81. Vermesh U, Vermesh O, Wang J, Kwong GA, Ma C, et al. 2011. High-density, multiplexed patterning of cells at single-cell resolution for tissue engineering and other applications. *Angew. Chem. Int. Ed.* 50:7378–80
82. Betts MR, Nason MC, West SM, De Rosa SC, Migueles SA, et al. 2006. HIV nonprogressors preferentially maintain highly functional HIV-specific CD8$^+$ T cells. *Blood* 107:4781–89
83. Morgan RA, Dudley ME, Wunderlich JR, Hughes MS, Yang JC, et al. 2006. Cancer regression in patients after transfer of genetically engineered lymphocytes. *Science* 314:126–29
84. Seder RA, Darrah PA, Roederer M. 2008. T-cell quality in memory and protection: implications for vaccine design. *Nat. Rev. Immunol.* 8:247–58
85. Ronan JL, Story CM, Papa E, Love JC. 2009. Optimization of the surfaces used to capture antibodies from single hybridomas reduces the time required for microengraving. *J. Immunol. Methods* 340:164–69
86. Bradshaw EM, Kent SC, Tripuraneni V, Orban T, Ploegh HL, et al. 2008. Concurrent detection of secreted products from human lymphocytes by microengraving: cytokines and antigen-reactive antibodies. *Clin. Immunol.* 129:10–18
87. Han Q, Bradshaw EM, Nilsson B, Hafler DA, Love JC. 2010. Multidimensional analysis of the frequencies and rates of cytokine secretion from single cells by quantitative microengraving. *Lab Chip* 10:1391–400
88. Varadarajan N, Kwon DS, Law KM, Ogunniyi AO, Anahtar MN, et al. 2012. Rapid, efficient functional characterization and recovery of HIV-specific human CD8$^+$ T cells using microengraving. *Proc. Natl. Acad. Sci. USA* 109:3885–90

89. Han Q, Bagheri N, Bradshaw EM, Hafler DA, Lauffenburger DA, Love JC. 2012. Polyfunctional responses by human T cells result from sequential release of cytokines. *Proc. Natl. Acad. Sci. USA* 109:1607–12
90. Mascher B, Schlenke P, Seyfarth M. 1999. Expression and kinetics of cytokines determined by intracellular staining using flow cytometry. *J. Immunol. Methods* 223:115–21
91. Ploegh HL. 1998. Viral strategies of immune evasion. *Science* 280:248–53
92. Kershaw MH, Westwood JA, Darcy PK. 2013. Gene-engineered T cells for cancer therapy. *Nat. Rev. Cancer* 13:525–41
93. Yaffe MB. 2013. The scientific drunk and the lamppost: massive sequencing efforts in cancer discovery and treatment. *Sci. Signal.* 6:pe13
94. Raj A, van Oudenaarden A. 2008. Nature, nurture, or chance: stochastic gene expression and its consequences. *Cell* 135:216–26
95. Paszek P, Ryan S, Ashall L, Sillitoe K, Harber CV, et al. 2010. Population robustness arising from cellular heterogeneity. *Proc. Natl. Acad. Sci. USA* 107:11644–49
96. Yuan TL, Wulf G, Burga L, Cantley LC. 2011. Cell-to-cell variability in PI3K protein level regulates PI3K-AKT pathway activity in cell populations. *Curr. Biol.* 21:173–83
97. Sisan DR, Halter M, Hubbard JB, Plant AL. 2012. Predicting rates of cell state change caused by stochastic fluctuations using a data-driven landscape model. *Proc. Natl. Acad. Sci. USA* 109:19262–67
98. Shin YS, Remacle F, Fan R, Hwang K, Wei W, et al. 2011. Protein signaling networks from single cell fluctuations and information theory profiling. *Biophys. J.* 100:2378–86
99. Nelson CM, Chen CS. 2002. Cell-cell signaling by direct contact increases cell proliferation via a PI3K-dependent signal. *FEBS Lett.* 514:238–42
100. Liu WF, Nelson CM, Pirone DM, Chen CS. 2006. E-cadherin engagement stimulates proliferation via RAC 1. *J. Cell Biol.* 173:431–41
101. Hui EE, Bhatia SN. 2007. Micromechanical control of cell–cell interactions. *Proc. Natl. Acad. Sci. USA* 104:5722–26
102. Puliafito A, Hufnagel L, Neveu P, Streichan S, Sigal A, et al. 2011. Collective and single cell behavior in epithelial contact inhibition. *Proc. Natl. Acad. Sci. USA* 109:739–44
103. Sear RP, Chung S-W, Markovich G, Gelbart WM, Heath JR. 1999. Spontaneous patterning of quantum dots at the air-water interface. *Phys. Rev. E* 59:R6255–58
104. Shao H, Chung J, Balaj L, Charest A, Bigner DD, et al. 2012. Protein typing of circulating microvesicles allows real-time monitoring of glioblastoma therapy. *Nat. Med.* 18:1835–40
105. Thery C, Ostrowski M, Segura E. 2009. Membrane vesicles as conveyors of immune responses. *Nat. Rev. Immunol.* 9:581–93
106. Al-Nedawi K, Micallef MB, Lhotak V, May L, Guha A, Rak J. 2008. Intercellular transfer of the oncogenic receptor EGFRvIII by microvesicles derived from tumour cells. *Nat. Cell Biol.* 10:619–24
107. Domon B, Aebersold R. 2006. Mass spectrometry and protein analysis. *Science* 312:212–17
108. Deutsch EW, Eng JK, Zhang H, King NL, Nesvizhskii AI, et al. 2005. Human plasma peptide atlas. *Proteomics* 5:3497–500
109. Charles P, Elliott MJ, Davis D, Potter A, Kalden JR, et al. 1999. Regulation of cytokines, cytokine inhibitors, and acute-phase proteins following anti-TNF-α therapy in rheumatoid arthritis. *J. Immunol.* 163:1521–28
110. Thornberry NA, Rano TA, Peterson EP, Rasper DM, Timkey T, et al. 1997. A combinatorial approach defines specificities of members of the caspase family and granzyme B. *J. Biol. Chem.* 272:17907–11
111. Weinstein IB, Joe A. 2008. Oncogene addiction. *Cancer Res.* 68:3077–3080
112. Neufeld G, Cohen T, Gengrinovitch S, Poltorak Z. 1999. Vascular endothelial growth factor (VEGF) and its receptors. *FASEB J.* 13:9–22